








ISSN: 2617-6548

URL: www.ijirss.com

The role of zincate morphology in electroless Ni-P deposition on AA5052 aluminum alloy

 Badrul Munir¹,  Vika Rizkia^{2*},  Iwan Susanto³,  Ade Utami Hapsari⁴,  Retna Deca Pravitasari⁵

¹Department of Metallurgical and Materials Engineering, Universitas Indonesia, Jl. Prof. Dr. Ir. R. Roosseno, Kampus Baru UI Depok, Depok 16425, Indonesia.

^{2,3}Department of Mechanical Engineering, Politeknik Negeri Jakarta, Jl Prof. Dr. G.A Siwabessy, Kampus Baru UI Depok, Depok 16425, Indonesia.

^{4,5}Research Center for Advanced Materials, National Research and Innovation Agency (BRIN), 224 Building, Area Science and Technology B.J.Habibie, South Tangerang 15314, Indonesia.

Corresponding author: Vika Rizkia (Email: vika.rizkia@mesin.pnj.ac.id)

Abstract

The growing need for lightweight aluminum alloys in transportation and aerospace demands advanced surface protection solutions. While electroless Ni-P coating offers excellent corrosion resistance, its performance critically depends on zincating pretreatment - a process whose multi-step optimization remains insufficiently studied. This study investigates the influence of single, double, and triple zincating on the morphology of zincate layers and their subsequent impact on the deposition of electroless Ni-P coatings. AA5052 underwent zincating treatments in 200 g/L NaOH + 10 g/L ZnO solution before electroless Ni-P deposition at 80°C (pH5) in nickel sulfate and sodium hypophosphite. Surface characterization was performed using FE-SEM/EDS, while electrochemical properties were evaluated through EIS in 0.5M H₂SO₄ solution. Key findings demonstrate that double zincating generates an optimal surface morphology, in form of porous microstructure (average pore size of 0.28µm), that enhances Ni-P nucleation. This morphology yields the highest Ni percentage, and corrosion resistance exhibiting the largest arc radius semicircle. Single zincating produces discontinuous deposits (0.33µm granules), while triple treatment creates over-smoothed surfaces compromising adhesion. The study concludes that the porous Zn layer from double zincating optimizes Ni-P coating adhesion and corrosion protection by providing mechanical anchoring sites, whereas excessive pretreatment diminishes nucleation efficacy.

Keywords: AA5052, Electroless Deposition, Ni-P, Porous Structure, Zincating.

DOI: 10.53894/ijirss.v8i6.10244

Funding: The studies and analysis were performed with the financial support of the International Collaboration Research Grant, Politeknik Negeri Jakarta No. 385/PL3.A.10/PT.00.06/2024 on 25th April 2024.

History: Received: 31 July 2025 / **Revised:** 2 September 2025 / **Accepted:** 5 September 2025 / **Published:** 26 September 2025

Copyright: © 2025 by the authors. This article is an open access article distributed under the terms and conditions of the Creative Commons Attribution (CC BY) license (<https://creativecommons.org/licenses/by/4.0/>).

Competing Interests: The authors declare that they have no competing interests.

Authors' Contributions: All authors contributed equally to the conception and design of the study. All authors have read and agreed to the published version of the manuscript.

Transparency: The authors confirm that the manuscript is an honest, accurate, and transparent account of the study; that no vital features of the study have been omitted; and that any discrepancies from the study as planned have been explained. This study followed all ethical practices during writing.

Publisher: Innovative Research Publishing

1. Introduction

In order to lower the energy consumption of transportation, aerospace, and other field, the modern world needs to adopt energy-saving measures. Therefore, utilizing new, cost-effective technologies and lightweight materials is crucial to attain this urgent objective [1, 2]. In this regard, owing to the superior workability and corrosion resistance, aluminum alloys are increasingly employed to enhance fuel efficiency by minimizing weight [3-5]. One of the most promising alloys is Al-Mg alloy, which possesses unique advantages such as lightweight, high formability, weldability, high strength, conductivity, and excellent processability [6-8]. Nevertheless, Al-Mg alloys demonstrate shortages in surface performance due to their inadequate corrosion resistance and mechanical properties in aggressive environments. Hence, it is crucial to implement a protective surface modification to enhance the corrosion resistance of Al-Mg alloys [9, 10].

Electroless deposition is an effective protective technique that results in a consistent coating with minimal porosity and excellent adhesion to the substrate. It is a simple, quick, and cost-efficient process. As a result, electroless coatings are widely utilized as a surface modification method for aluminum to prevent corrosion [8, 11]. Electroless nickel coatings have become increasingly popular as a result of their high hardness, as well as their exceptional resistance to wear, abrasion, and corrosion on aluminum alloys [12, 13]. Previous research has demonstrated that electroless nickel alloys can enhance the strength, tribo-mechanical properties, and corrosion resistance of aluminum substrates [14-17]. Furthermore, electroless nickel surpasses other protective coatings in terms of thickness uniformity and conformity to complicated shapes [18]. However, the adhesion between coatings and underlying substrates is decreased by the highly stable and rapid formation of an oxide layer on the aluminum surface. Therefore, specific pretreatments are required prior to nickel coating on aluminum alloy [13, 19, 20].

Zincating is the most practical and satisfactory method of aluminum preparation before further deposition [21-23]. Zincating represents an electrochemical exchange reaction involving zinc complexes within the solution and the aluminum substrate, resulting in the deposition of zinc crystallites through the dissolution of aluminum. The deposition of zinc serves to safeguard the surface, thereby establishing a robust foundation for any subsequent layers of deposition. To enhance the adhesion strength of the Zn layer, it is advantageous to employ a multiple immersion zincating operation [4].

Nevertheless, the prevailing method employed on Al-Mg and other aluminum alloys is the double zincating process. Although the multisteps zincating method of the substrate plays a crucial role in determining the morphology and the properties of electroless Ni-P coatings on aluminum alloys, there is a notable scarcity of published research addressing this topic. This study aims to bridge this knowledge gap by systematically investigating the impact of single, double, and triple zincating treatments on the morphology of the zincate layer and its subsequent effect on the characteristics of electroless Ni-P coatings deposited on AA5052 aluminum alloy.

2. Materials and Methods

2.1. Materials

Square specimens of commercially AA5052 aluminum alloy, measuring 1.5 cm x 1.5 cm, were used in this study. The specimens were initially subjected to a mechanical polishing process using a series of abrasive papers with grit sizes ranging from 100 to 1500. Following polishing, the specimens were thoroughly rinsed with distilled water, then degreased in a 5% NaOH solution at 50°C for 3 minutes. After a preliminary cleaning in acetone for 30 seconds, AA5052 was acid-stripped for 1 minute in a 1M H₂SO₄ solution.

2.2. Zincating Pretreatment

The AA5052 substrates were subjected to a zincating pretreatment process to enhance the adhesion of the subsequent Ni-P coating. Zincating was performed using a solution containing 200 g/L NaOH and 10 g/L ZnO at room temperature. Three different zincating procedures were employed: single, double, and triple immersion, each with an immersion time of 2 minutes. For the double and triple zincating procedures, the AA5052 substrates were rinsed with deionized water and immersed in a 1 M H₂SO₄ solution for 1 minute between each immersion step.

2.3. Ni-P Deposition

The final step is the electroless deposition of Ni-P on the zincated specimens. The coating process was carried out in a solution containing 30 g.L⁻¹ nickel sulfate as a source of nickel, 20 g.L⁻¹ sodium hypophosphite as a source of phosphorus and reducing agent, and 20 g.L⁻¹ sodium citrate as a complexing ligand. The solution was maintained at 80°C and pH 5 for 60 minutes.

2.4. Morphological Analysis

The surface morphology and elemental distribution of Ni-P coated AA5052 were examined using Field Emission Scanning Electron Microscopy FEI Inspect F50. It is equipped with EDS analysis to determine the chemical composition of the coatings. The composition of the coating was investigated through energy dispersive spectroscopy (EDS) analysis.

2.5. Electrochemical Analysis

EIS is conducted to determine the resistance of zincating surfaces and Ni-P layers by immersion in a solution of 0.5 M H₂SO₄ with O₂ bubbles at room temperature. The EIS is carried out using a conventional three-electrode cell assembly: AA5052 as a working electrode, graphite as a counter electrode, and Standard Calomel Electrode (SCE) as a reference electrode. This test is conducted in the frequency range of 100 kHz-0.01 Hz.

3. Results and Discussions

3.1. Analysis of Zinc Deposits

The immersion of aluminum within an alkaline zincate solution initiates a redox reaction at the aluminum-solution interface. This zincate process can be characterized by two distinct electrochemical reactions occurring at separate sites on the aluminum surface: anodic dissolution of aluminum and cathodic reduction of zinc. The chemical reactions underpinning the zincate immersion process can be represented as follows [24, 25]:

The anodic reaction comprises the dissolution of the aluminum substrate,



While the cathodic reaction involves the reduction of zinc ions from the alkaline zincate solution,



This galvanic coupling between the aluminum and the zincate solution results in the deposition of zinc particles onto the aluminum surface,

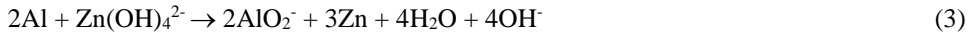
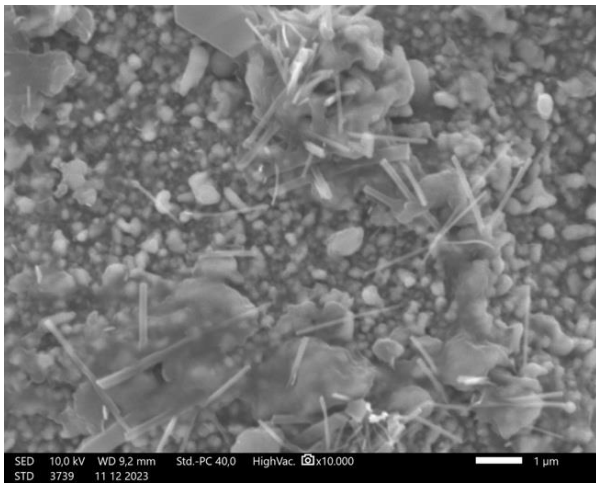
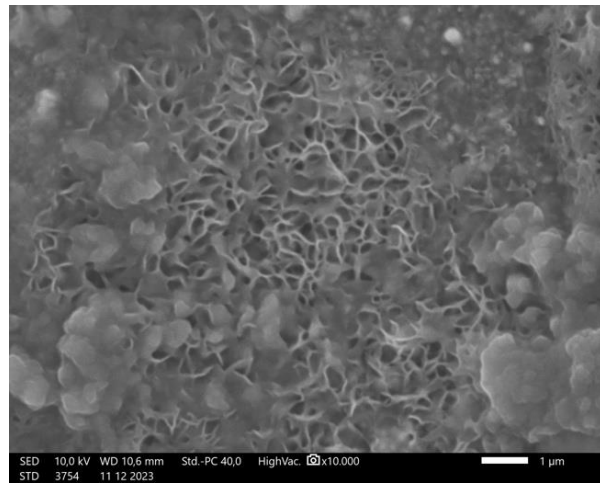


Figure 1. and Table 1 depict the FE-SEM pictures and EDS analysis of AA5052 following various zincate pretreatment methods, comprising single, double, and triple treatments. As indicated in the images, all zincate treatments resulted in noticeable zinc deposition on the AA5052 surface. Due to the interaction of chemical dissolution (by acidic solution) and galvanic replacement in the zincate bath, variations in morphology were observed depending on the number of zincate treatments applied.

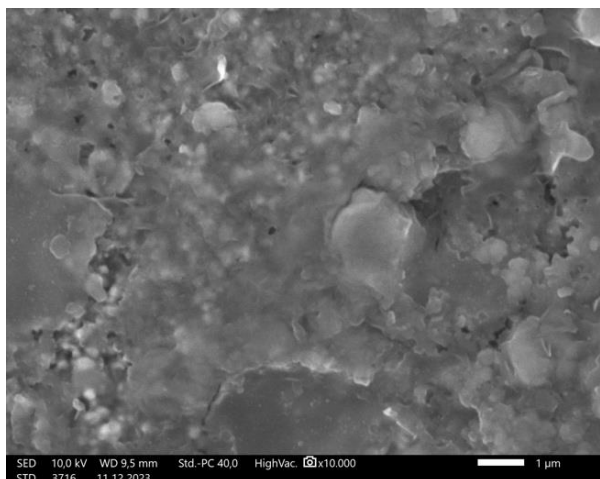
Figure 1a. depicts the surface of AA5052 subsequent to a single zincating treatment. The zinc deposit exhibits a non-uniform and heterogeneous morphology, characterized by a varied distribution of particle sizes. Both larger agglomerated clusters and smaller granular particles are observed. The agglomerated clusters are not densely packed, indicating inhomogeneous surface coverage. ImageJ analysis revealed an average diameter of 0.33 μm for the granular particles. This inhomogeneous phenomenon may be attributed to the uneven surface of the AA5052 substrate resulting from the acid-cleaning process. Lee, et al. [26] in their research showed a correlation between zinc nucleation sites and both surface roughness and electrochemical properties. The initial stage of zinc deposition is characterized by the preferential formation of zinc clusters on convex regions of the aluminum surface, corresponding to peaks and edges. While aluminum dissolution occurs across the entire substrate, the high conductivity of the aluminum facilitates electron transport, promoting zinc reduction and deposition at these convex sites. Moreover, convex areas benefit from shorter diffusion paths for zinc ions from the zincate solution, further enhancing deposition. In addition, distinct needle-like structures with an average length of 2.16 μm are observed, suggesting the presence of crystalline zinc phases.



(a)



(b)



(c)

Figure 1.

SEM images of AA5052 aluminum alloy surfaces subjected to (a) single, (b) double, and (c) triple zincate treatments.

Figure 1b. reveals a porous morphology, with an average pore diameter of 0.28 μm, on the double zincated AA5052 surface. This morphology is primarily attributed to the dissolution of Zn nuclei after acid stripping on H₂SO₄. A closer examination of the image highlights a sub-surface porous microstructure interspersed with open pores. This phenomenon likely arises from the leaching of both underlying and overgrown Zn deposits. Furthermore, Zn deposits exhibit greater thickness in regions adjacent to porous areas. Under conditions of pronounced surface irregularities such as deep cavities and porous, zinc ion diffusion is significantly hindered. Nevertheless, the anodic dissolution of aluminum and cathodic reduction of zinc ions continues at a considerably fast rate, leading to the localized growth of large zinc deposits adjacent to the porous structure.

Figure 1c. illustrates the surface morphology of the Zn deposit formed after a triple zincating treatment. The zinc coating exhibits a relatively uniform coverage across the substrate surface, with most of the substrate area being covered by the deposit. The surface displays a smooth texture composed of the fusion of granular structures. The zinc deposits effectively seal the porous morphology through overlapping layers of zinc, resulting in enhanced surface coverage and uniformity.

Table 1.

The EDS results of AA5052 aluminum alloy surfaces subjected to (a) single, (b) double, and (c) triple zincate treatments.

Treatment	Al (wt.%)	Zn (wt.%)	Al (at.%)	Zn (at.%)
Single Zincate	54.14 ± 0.09	45.86 ± 0.26	74.09 ± 0.13	25.91 ± 0.15
Double Zincate	63.21 ± 0.08	36.79 ± 0.20	80.63 ± 0.11	19.37 ± 0.11
Triple Zincate	62.26 ± 0.10	37.74 ± 0.24	79.99 ± 0.13	20.01 ± 0.13

EDS analysis, as seen in Table 1, reveals an approximate 18% reduction in zinc content between the single and subsequent double or triple zincate treatments. This observation suggests that repeated zincating cycles, despite increasing the overall zinc deposition, might not necessarily translate to a thicker coating. According to Pachchigar, et al. [4] possible contributing factor is the galvanic overpotential during single zincating is higher than in double and triple zincating. This higher overpotential drives a faster initial deposition rate, leading to a thicker zinc layer in the single zincating process. In double and triple zincating, the overpotential is lower, resulting in a slower deposition rate and thinner layers.

3.2. Analysis of Nickel Deposits

According to the mechanism proposed by Brenner and Riddell, the so-called electrochemical mechanism, the chemical reactions elucidate the Ni-P electroless deposition process on zincated AA5052 can be represented as follow:

An anodic reaction involves the generation of electrons through the interaction of water and hypophosphite [27] :



Cathodic reactions that utilize the electrons produced in (4)



Figure 2 displays scanning electron microscopy (SEM) images of the zincated AA5052 surface after undergoing Ni-P electroless deposition. As depicted in Figure 2a and c the substrate undergoing single and triple zincating exhibits a dual morphological regime: uniformly distributed nodular structures with prominent crater-like formations. However, Figure 2b shows a different morphology with no crater formation, the Ni-P deposits were observed predominantly on the AA5052 substrate subjected to double zincating. The deposit exhibits a characteristic spheroidal nodular morphology, with

individual nodules averaging 0.47 μm in diameter. Furthermore, these nodules aggregated into coalesced clusters, measuring approximately 2.1 μm in average diameter, indicative of progressive growth and interfacial merging during deposition. The resulting Ni layer exhibited a non-uniform and non-continuous morphology.

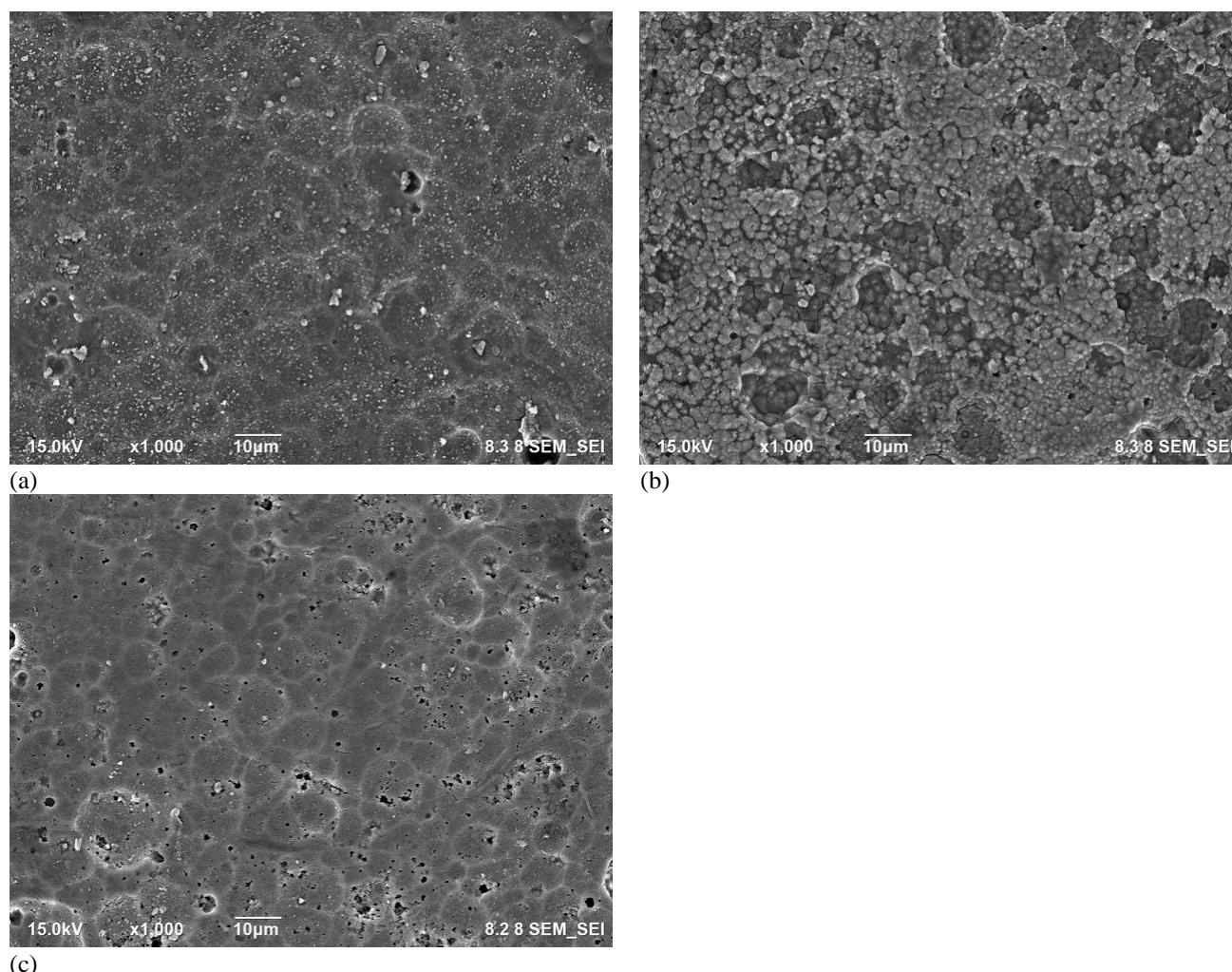


Figure 2. SEM micrographs with corresponding EDS analysis of the AA5052 surface after (a) single, (b) double, and (c) triple zincating, followed by Ni-P electroless deposition.

Energy-dispersive X-ray spectroscopy (EDS) analysis, as seen in Table 2, reveals a lower percentage of Zn on the AA5052 surface after Ni-P deposition. This observation suggests that the electroless Ni-P deposition process on AA5052 involves not only the oxidation of hypophosphite but also the oxidation and dissolution of the Zn deposit in anodic sites with the reaction of :



This finding aligns with the observations of Court, et al. [24] which reported the dissolution of the Zn layer prior to electroless Ni-P deposition on aluminum substrates, accompanied by a shift towards a less negative potential. Furthermore, the dissolution of the Zn layer in this study likely compromises the adhesion of the Ni-P coating on the AA5052 surface, potentially by disrupting the formation of a robust interface between the aluminum substrate and the Ni-P deposit. This compromised adhesion could result in a reduction in the catalytic activity necessary for efficient Ni-P deposition.

Moreover, Table 2 demonstrates a marked increase in Ni content between single and double zincating processes, which notably correlates with enhanced Ni-P layer deposition following double zincating process. However, Ni content drops dramatically after the triple zincate treatment. This study reveals that the morphology of the Zn nuclei, whether rough, smooth, or dense, does not solely dictate the effectiveness of subsequent electroless Ni-P plating and adhesion on AA5052. Instead, the effectiveness of the Ni-P deposition process on zincate-pretreated Al5052 alloy is primarily attributed to the distinctive porous structure of the zincate layer. This hierarchical, porous architecture provides a significantly larger surface area compared to a conventional Zn immersion layer, which is crucial for mechanical interlocking sites during the deposition process. This result aligns with the finding of Zhai, et al. [28] which reported that substrate surface morphology is a critical determinant of Ni-P coating adhesion. Their work demonstrated that after electroless deposition, a compact Ni-P coating was embedded into the porous network.

Table 2.

The EDS results of AA5052 aluminum alloy surfaces subjected to (a) single, (b) double, and (c) triple zincate treatments.

Treatment	Al (wt%)	Zn (wt%)	Ni (wt%)	Al (at%)	Zn (at%)	Ni (at%)
Single Zincate	76.7 ± 0.1	5.9 ± 0.1	17.5 ± 0.1	88.6 ± 0.1	3.1 ± 0.1	8.3 ± 0.1
Double Zincate	67.1 ± 0.1	2.5 ± 0.1	30.4 ± 0.1	81.7 ± 0.1	1.3 ± 0.1	17.0 ± 0.1
Triple Zincate	96.0 ± 0.1	1.6 ± 0.1	2.4 ± 0.1	98.2 ± 0.1	0.7 ± 0.13	1.1 ± 0.1

Scanning electron microscopy analysis, as depicted in Figure 3 revealed the formation of intergranular cracks within the zincate layer on the AA5052 substrate subsequent to its immersion in the electroless Ni-P plating solution. This phenomenon implies that the chemical interaction occurring at the interface between the zincate film and the Ni-P plating bath generated internal stresses sufficient to induce the crack of the zincate layer. Notably, The SEM image reveals that the Ni-P deposit does not grow within the cracks and adjacent to them on the zincated AA5052 surface. This phenomenon can be attributed to the characteristics of the cracks and their influence on the electroless deposition process. The cracks in the zincated AA5052 substrate may act as localized anodic sites with increased reactivity due to stress concentration and exposed edges. Therefore, making them less favorable for nickel deposition. Furthermore, the galvanic coupling between the more active zincated AA5052 and the less active nickel may make the displacement reaction between the anodic zincated aluminum and cathodic nickel ions in the electroless bath proceeds at a significantly high rate near the cracks. As a result, large nickel particles are preferentially formed near the cracks due to the localized high concentration of nickel ions and the rapid deposition kinetics.

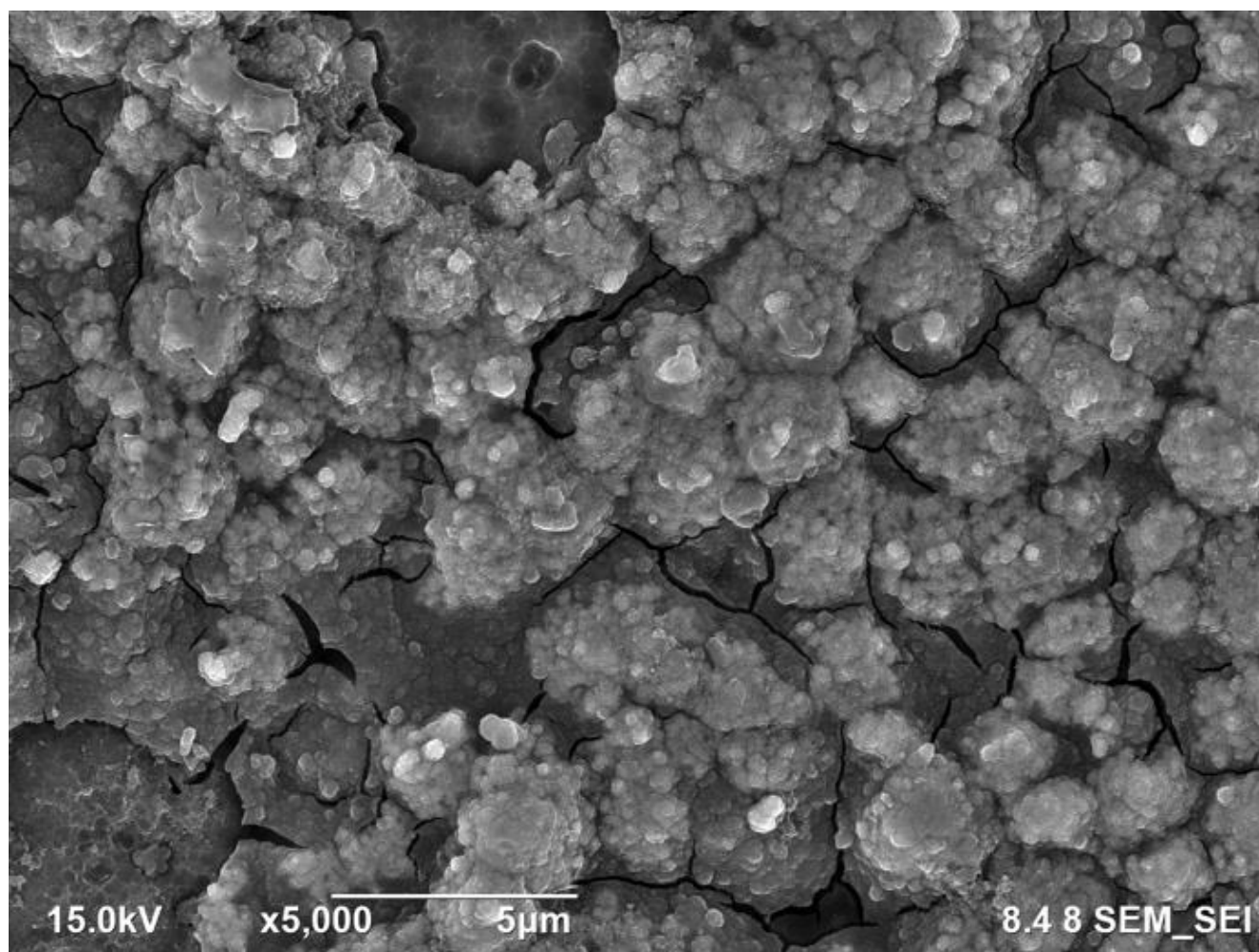


Figure 3. Scanning electron microscopy (SEM) image of the double zincated AA5052 surface after Ni-P deposition. The image is taken at a magnification of 5000x and highlights the formation of cracks within the Zn layer.

3.3. Electrochemical Behaviour of Ni-P/AA5052 with Various Zincating Pretreatments

Figure 4 displays the Nyquist plots measured at open-circuit potential (OCP) for bare AA5052 and Ni-P/AA5052 substrates subjected to single, double, and triple zincating pretreatment. The impedance spectra were interpreted using an equivalent electrical circuit model (shown in the figure inset), consisting of solution resistance (R_s), multiple charge transfer resistances (R_1 – R_5), constant phase elements (CPE_1 , CPE_2), and an inductance (L_1) which accounts for the observed inductive loop at low frequencies.

The plots exhibit one semicircular arc, which is a combination of high-frequency and medium-frequency arcs, followed by a low-frequency inductive loop, indicating complex interfacial processes. The high-frequency arc is typically attributed to the response of the Ni-P coating layer, while the medium-frequency arc corresponds to the double layer and charge transfer resistance at the substrate/ Ni-P interface.

The presence of an inductive loop suggests adsorption/desorption processes or localized corrosion phenomena such as pitting, which are frequently observed in systems involving passive layer breakdown on aluminum alloys. The consistent appearance of this feature across all samples may reflect: (i) inhomogeneous Ni-P deposition characteristics, and (ii) intergranular cracking in the zincate layer that facilitates substrate pitting. Moreover, the occurrence of intergranular cracks in the zincate layer, particularly after the Ni-P deposition process (Figure 3), highlights stress-induced failure points that compromise coating uniformity and could serve as electrochemical weak spots.

Electrochemical impedance spectroscopy revealed distinct performance variations among the coated samples. The double zincate/Ni-P treated AA5052 exhibited the largest capacitive arc diameter in Nyquist plots, demonstrating the highest polarization resistance and consequently, the most effective corrosion protection. In contrast, both single and triple zincate specimens showed impedance responses comparable to uncoated AA5052, indicating negligible improvement in corrosion resistance. These electrochemical findings align precisely with the EDS results, which revealed a significant increase in Ni content from single to double zincating, indicative of a substantially greater deposition of the Ni-P layer after the double zincate treatment. Moreover, it was observed that the Ni content sharply decreased following the triple zincate treatment, correlating with the diminished corrosion protection.

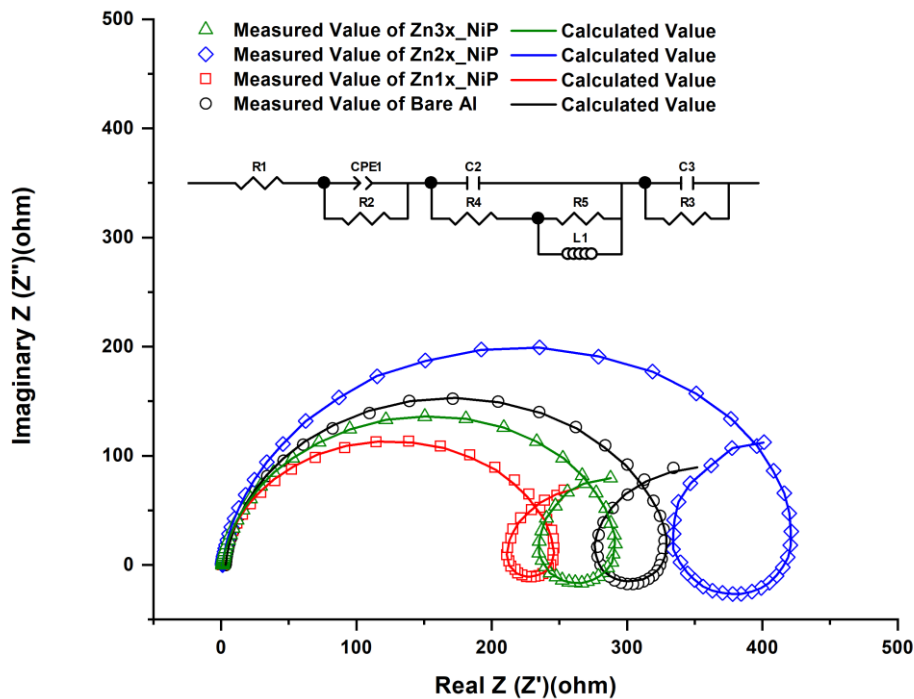


Figure 4. Nyquist curves of the AA5052 surface after single, double, and triple zincating, followed by Ni-P electroless deposition.

The close agreement between the measured data (symbols) and the simulated curves (solid lines) supports the validity of the chosen equivalent circuit model. The differences in impedance behavior among the coated samples highlight the critical role of zincating steps as a pretreatment Ni-P deposition, in determining protective performance. In particular, double zincating appears to offer an optimal balance between barrier protection and electrochemical stability, likely due to the distinctive porous structure of the zincate layer, which facilitates enhanced Ni nucleation and adhesion. This surface morphology promotes a higher percentage of Ni incorporation on the substrate surface during subsequent electroless plating.

4. Conclusion

This study elucidates the critical relationship between zincate pretreatment morphology and the resulting characteristics of electroless Ni-P coatings on AA5052 aluminum alloy, demonstrating that the structural evolution of the zincate layer directly governs coating adhesion, and corrosion performance. Three key findings emerge from systematic comparisons of single, double, and triple zincating processes:

- Single zincating generated discontinuous granular Zn deposits (0.33 μm avg. diameter) with faceted clusters, a consequence of substrate heterogeneities due to acid cleaning. In contrast, double zincating produced a hierarchically

porous microstructure (0.28 μm avg. diameter) through selective Zn dissolution during acid stripping. This morphology provided both increased surface area and mechanical interlocking sites, whereas triple zincating, despite improved macroscopic uniformity, yielded the lowest Zn percentage.

- The porous zincate layer from double zincating facilitated optimal Ni-P deposition, evidenced by dense, spheroidal nodular coatings (0.47 μm avg. nodule diameter) with maximal Ni content. This contrasts with the single zincating (crater formation due to uneven Zn coverage) and triple zincating (insufficient nucleation sites from excessive smoothing). The double-zincated substrate's superior performance arises from its porous morphology, which provided greater surface area and mechanical interlocking sites.
- EIS revealed that the double-zincated/Ni-P coating achieved the highest corrosion protection, exhibiting the largest capacitive arc in EIS Nyquist plots, attributed to optimal barrier protection and electrochemical stability

References

- [1] Z. Sharifalhosseini and A. Davoodi, "Uniform nucleation of zincate layer through the optimized etching process to prevent failure in electroless plating on 2024 aluminum alloy," *Engineering Failure Analysis*, vol. 124, p. 105326, 2021. <https://doi.org/10.1016/j.engfailanal.2021.105326>
- [2] U. Idrees *et al.*, "Finite element analysis of car frame frontal crash using lightweight materials," *Journal of Engineering Research*, vol. 11, no. 1, p. 100007, 2023. <https://doi.org/10.1016/j.jer.2023.100007>
- [3] Y. Wang *et al.*, "Influence of pretreatments on physicochemical properties of Ni-P coatings electrodeposited on aluminum alloy," *Materials & Design*, vol. 197, p. 109233, 2021. <https://doi.org/10.1016/j.matdes.2020.109233>
- [4] V. Pachchigar, J. Varshney, S. K. Ghosh, and V. Kain, "Reinvestigation of nucleation and growth of Zn on Al surface during modified alloy zincating," *Surface and Coatings Technology*, vol. 382, p. 125191, 2020. <https://doi.org/10.1016/j.surfcoat.2019.125191>
- [5] A. Candela, G. Sandrini, M. Gadola, D. Chindamo, and P. Magri, "Lightweighting in the automotive industry as a measure for energy efficiency: Review of the main materials and methods," *Heliyon*, vol. 10, no. 8, p. e29728, 2024. <https://doi.org/https://doi.org/10.1016/j.heliyon.2024.e29728>
- [6] Y. Zeng, Z. He, Q. Hua, Q. Xu, and Y. Min, "Polyacrylonitrile infused in a modified honeycomb aluminum alloy bipolar plate and its acid corrosion resistance," *ACS Omega*, vol. 5, no. 27, pp. 16976-16985, 2020. <https://doi.org/10.1021/acsomega.0c02742>
- [7] Z. Qin, Y. Zeng, Q. Hua, Q. Xu, X. Shen, and Y. Min, "Synergistic effect of hydroxylated boron nitride and silane on corrosion resistance of aluminum alloy 5052," *Journal of the Taiwan Institute of Chemical Engineers*, vol. 100, pp. 285-294, 2019. <https://doi.org/10.1016/j.jtice.2019.04.029>
- [8] L. Yang, Y. Wan, Z. Qin, Q. Xu, and Y. Min, "Fabrication and corrosion resistance of a graphene-tin oxide composite film on aluminium alloy 6061," *Corrosion Science*, vol. 130, pp. 85-94, 2018. <https://doi.org/10.1016/j.corsci.2017.10.031>
- [9] J. Gu, X. Zhang, and L. Yu, "Investigation on anodized 5052 aluminum alloy and its corrosion resistance in simulated acid rain," *International Journal of Electrochemical Science*, vol. 18, no. 11, p. 100336, 2023. <https://doi.org/10.1016/j.ijoes.2023.100336>
- [10] H. Wang, S. Chang, Z. Zhou, and W. Wang, "Effect of TIG remelting on the microstructure, mechanical properties, and corrosion behavior of 5052 aluminum alloy joints in MIG welding," *Journal of Materials Research and Technology*, vol. 32, pp. 2255-2267, 2024. <https://doi.org/10.1016/j.jmrt.2024.08.087>
- [11] Q. Yuan *et al.*, "Corrosion resistance of superhydrophobic Ni-B/TiC composite coatings prepared by electroless deposition," *Colloids and Surfaces A: Physicochemical and Engineering Aspects*, vol. 702, p. 135023, 2024. <https://doi.org/10.1016/j.colsurfa.2024.135023>
- [12] P. Vetrivezhan, C. Ayyanar, P. V. Arunraj, P. Vasanthkumar, and D. Ganesan, "Electroless deposition of aluminium alloy LM25 by SiC and Ni-P nano coating," *Materials Today: Proceedings*, vol. 45, pp. 6449-6453, 2021. <https://doi.org/10.1016/j.matpr.2020.11.280>
- [13] M. Sundararajan, M. Devarajan, and M. Jaafar, "Electroless Ni-B sealing on nanoporous anodic aluminum oxide pattern: Deposition and evaluation of its characteristic properties," *Journal of Materials Research and Technology*, vol. 19, pp. 4504-4516, 2022. <https://doi.org/10.1016/j.jmrt.2022.06.169>
- [14] Z. Qian, Z. Luo, Y. Dong, L. Yao, R. Song, and Y. Xu, "Tribological behavior and surface analysis of electroless nickel coatings reinforced with black phosphorus nanosheets," *Tribology Transactions*, vol. 66, no. 2, pp. 268-278, 2023. <https://doi.org/10.1080/10402004.2023.2171930>
- [15] M. Köse *et al.*, "Improving the tribological and corrosion behavior of NiB coating with low boron content from optimized lead-free bath on aluminum alloys," *Surface and Coatings Technology*, vol. 494, p. 131464, 2024. <https://doi.org/10.1016/j.surfcoat.2024.131464>
- [16] H. Gul, H. Algul, A. Akyol, M. Uysal, and A. Alp, "Evaluation of wear and corrosion behavior of electroless Ni-B-P/CNT composite coatings on aluminum surfaces," *Diamond and Related Materials*, vol. 137, p. 110075, 2023. <https://doi.org/10.1016/j.diamond.2023.110075>
- [17] R. Jeevanantham and D. Nagaraju, "Impact of electroless Ni-P coated pumice particles on the mechanical properties of scrap aluminium metal matrix composites," *Materials Letters*, vol. 377, p. 137491, 2024. <https://doi.org/10.1016/j.matlet.2024.137491>
- [18] V. Vitry, J. Hastir, A. Mégret, S. Yazdani, M. Yunacti, and L. Bonin, "Recent advances in electroless nickel-boron coatings," *Surface and Coatings Technology*, vol. 429, p. 127937, 2022. <https://doi.org/10.1016/j.surfcoat.2021.127937>
- [19] V. Skryabin and A. Skhirtladze, "Formation of a nickel-phosphorus coating on aluminum alloy parts," *Russian Metallurgy* vol. 2021, no. 13, pp. 1677-1680, 2021. <https://doi.org/10.1134/S0036029521130280>
- [20] B. Wang, J. Li, Z. Xie, G. Wang, and G. Yu, "High corrosion and wear resistant electroless Ni-P gradient coatings on aviation aluminum alloy parts," *International Journal of Minerals, Metallurgy and Materials*, vol. 31, no. 1, pp. 155-164, 2024. <https://doi.org/10.1007/s12613-023-2689-3>

- [21] Z. Yin and F. Chen, "A facile electrochemical fabrication of hierarchically structured nickel–copper composite electrodes on nickel foam for hydrogen evolution reaction," *Journal of Power Sources*, vol. 265, pp. 273-281, 2014. <https://doi.org/10.1016/j.jpowsour.2014.04.123>
- [22] I. Othman, M. Starink, and S. Wang, "Electrodeposition of nickel coating on aa7075 substrate via modified single zincating method with assistance of copper activation," *Journal of Advanced Manufacturing Technology*, vol. 14, no. 2, pp. 75–86, 2020.
- [23] H.-Z. Liu, S.-P. Chen, and W.-W. Zhang, "Effect of double zincating on microstructures and bonding strength of coatings on aluminum alloy for pulse gold plating," *Heliyon*, vol. 10, no. 22, p. e40438, 2024. <https://doi.org/10.1016/j.heliyon.2024.e40438>
- [24] S. Court, C. Kerr, C. Ponce de León, J. R. Smith, B. D. Barker, and F. C. Walsh, "Monitoring of zincate pre-treatment of aluminium prior to electroless nickel plating," *Transactions of the IMF*, vol. 95, no. 2, pp. 97-105, 2017. <https://doi.org/10.1080/00202967.2016.1236573>
- [25] N. R. Paluvai, H. Hafeez, D.-H. Han, H.-Y. Ryu, C.-S. Lee, and J.-G. Park, "Preparation of a high hydrophobic aluminium surface by double zincating process," *Journal of Adhesion Science and Technology*, vol. 31, no. 10, pp. 1061-1074, 2017. <https://doi.org/10.1080/01694243.2016.1244035>
- [26] S.-K. Lee, J.-H. Lee, and Y.-H. Kim, "Nucleation and growth of zinc particles on an aluminum substrate in a zincate process," *Journal of Electronic Materials*, vol. 36, no. 11, pp. 1442-1447, 2007. <https://doi.org/10.1007/s11664-007-0280-8>
- [27] G. O. Mallory and J. B. Hajdu, *Electroless plating: Fundamentals and applications*. Cambridge, UK: Cambridge University Press, 1990.
- [28] T. Zhai, J. Chen, B. Gui, Q. Wang, and D. a. Yang, "Electroless deposition of Ni-P on poly (ether ether ketone)/multi-walled carbon nanotubes composite and improvement of the electrical conductivity in direction of thickness," *Journal of The Electrochemical Society*, vol. 162, no. 14, p. D613, 2015. <https://doi.org/10.1149/2.0591514jes>